EFFECTIVENESS FACTOR FOR A NON-ISOTHERMAL SIMPLE CATALYTIC REACTION WITH COMBINED TRANSPORT PROCESSES: MAXWELL–STEFAN APPROACH

Petr SCHNEIDER

Institute of Chemical Process Fundamentals, Academy of Sciences of the Czech Republic, 165 02 Prague 6-Suchdol, Czech Republic; e-mail: schneider@icpf.cas.cz

A two-step procedure is developed and tested for the prediction of effectiveness factors for stoichiometrically simple catalytic reactions. In the first step the dependences of state variables (concentrations, temperature, pressure) on the concentration of the key reaction component is obtained. The knowledge of these dependences allows then all the dependent variables in the catalyst pellet mass and heat balances to be expressed by this concentration. In the second step, a single balance differential equation is solved and the effectiveness factor is obtained. In addition, a deeper insight into the concentration and temperature conditions inside the pores is gained. Information of this kind can cast light on some features of the catalytic reactor behaviour. The analysis of ammonia synthesis illustrates this point.
Key words: Pore diffusion; Effectiveness factor; Maxwell–Stefan diffusion; Ammonia synthesis.

The constitutive equation that forms the basis of the largest part of the extensive literature on the prediction of effectiveness of porous catalysts is the Fick law[1–5]. This law assumes direct proportionality between the diffusion flux contribution for a component and the composition gradient of this component. In porous solids, such a law is correct only for binary diffusion on condition that diffusion is purely of the bulk or Knudsen type. Since all actually important catalytic reactions are multicomponent and pore diffusion takes place usually in the transition diffusion region, the application of the Fick law can be considered only as a rough approximation.

This problem can be solved by the application of the modified Maxwell–Stefan diffusion equation (see, *e.g.*, ref.[6]) which accounts for both the multicomponent character of reaction mixtures as well as for the transition diffusion mechanism[7,8].

It is the aim of this contribution to show how the problem of the catalyst effectiveness prediction, in which the combined mass transport due to composition gradients (diffusion; described by the modified Maxwell–Stefan equation) and pressure gradient (permeation; described by the Weber equation) can be simply solved for stoichiometrically simple reactions. As an illustration, the proposed method is applied to the high-temperature, high-pressure ammonia synthesis. Since the transport parameters of the

commonly used promoted iron catalyst are not available, arbitrary values were used. This prevents, however, direct comparison of the obtained results with experiments.

PROBLEM FORMULATION

To predict the influence of mass and heat transport in porous catalysts on the rate of heterogeneous reactions, it is necessary to solve the differential mass balances of reaction mixture components together with the heat balance. For simple geometric shapes of catalyst pellets (infinite slab $w = 0$, infinite cylinder $w = 1$, sphere $w = 2$) and a simple reaction with n reaction components

$$\sum_{i=1}^{n} a_i A_i = 0 \tag{1}$$

(stoichiometric coefficients $a_i > 0$ for reaction products, $a_i < 0$ for reactants and $a_i = 0$ for inert components), these balances have the following form:

$$\frac{1}{z^w} \frac{d}{dz}(z^w N) = -R(c,T) \ , \tag{2}$$

$$\frac{1}{z^w} \frac{d}{dz}(z^w Q/T_s) = -\frac{(-\Delta H_r)R_1}{T_s a_1} \ . \tag{3}$$

Here z is the geometric coordinate from the centre ($z = 0$) to the outer surface of the porous pellet ($z = R$), R is the radius of the sphere or infinite cylinder or the half-thickness of an infinite slab, $c = [c_1, c_2, ..., c_n]^T$ is the vector of molar concentrations of reaction components and N is the vector of molar flux densities of reaction mixture per unit total cross-section of the pellet, $N = [N_1, N_2, .., N_n]^T$, and R is the vector of *rates of formation* of reaction components per unit volume of the catalyst pellet, $R = [R_1, R_2, ..., R_n]^T$. Concentration- and temperature-dependent components of this vector, R_i, are related to the (always positive) reaction rate, r (*i.e.* moles of reaction (*1*) turnovers) per unit volume of the porous catalyst

$$R_i = a_i r \ . \tag{4}$$

Thus, R_i is positive for reaction products ($a_i > 0$; rate of formation) and negative for reactants ($a_i < 0$; rate of disappearance). Q is the heat flux density per unit total cross section of the pellet, due to the heat of reaction (*1*), ΔH_r (Joule per mole of reaction (*1*) turnovers), T_s is the pellet surface temperature.

Sign convention: If temperature or a component concentration decreases from the outer pellet surface ($z = R$) toward the pellet centre ($z = 0$), the corresponding flux density, N_i or Q, is directed toward the pellet interior and is positive.

Using the Maxwell–Stefan approach in formulation of combined gas transport due to composition and pressure gradients in multicomponent gas mixtures, the constitutive equations, which relate the flux densities N to the driving forces dc/dz can be formulated for two models of porous medium, *viz.* the Mean Transport–Pore Model (MTPM) and Dusty–Gas Model (DGM) in the following way:

$$\frac{dc}{dz} = FN \ . \tag{5}$$

The elements of $n*n$ matrix $F = \{f_{ij}\}$ for MTPM and DGM are shown in Appendix 1.

To obtain the profiles of concentrations of reaction mixture components, $c_i(z)$ ($i = 1,\ldots, n$), and temperature, $\theta(z)$, it is necessary to solve the system of ($n + 1$) coupled ordinary differential equations (6) and (7) obtained by combining Eqs (2) and (5), and Eq. (3) with the Fourier law $Q = \lambda \, dT/dz$:

$$\frac{1}{z^w} \frac{d}{dz}\left(z^w F^{-1} \frac{dc}{dz} \right) = R \ , \tag{6}$$

$$\frac{1}{z^w} \frac{d}{dz}\left(z^w \lambda \frac{d\theta}{dz} \right) = -\frac{(-\Delta H_r)}{T_s a_1} \ . \tag{7}$$

Here, λ denotes the effective heat conductivity of the porous catalyst and $\theta \equiv T/T_s$ where T_s is the temperature at the outer surface of the catalyst pellet ($T(R) = T_s$).

The boundary conditions of the system (6), (7) follow from

1. the symmetry of the concentration and temperature fields

$$\text{at } z = 0: \qquad dc/dz = 0 \ ,$$
$$d\,\theta/dz = 0 \ , \tag{8}$$

2. the known concentrations and temperature at the pellet outer surface

$$\text{at } z = R: \qquad c = c_s \ ,$$
$$\theta = 1 \ , \tag{9}$$

c_s represents the vector of molar concentrations of a reaction mixture component at the outer catalyst surface ($c(R) = c_s$).

This is the $(n + 1)$-dimensional split boundary value problem which has to be solved iteratively. Even though standard algorithms exist for this purpose, repeated solution, *e.g.*, for changing bulk gas composition and temperature along an integral reactor, presents an unpleasant numerical problem. Additional complication is introduced by the necessity of inverting matrix F in each integration step.

Solution of the multidimensional boundary value problem can be, however, circumvented by taking into account the stoichiometry of reaction (*1*) and splitting the solution into two steps.

TWO-STEP SOLUTION METHOD

First Step

Obviously, the molar flux densities, N_i, are coupled by the reaction stoichiometry (*1*)

$$\frac{N_i}{a_i} = \frac{N_j}{a_j} \ , \quad i, j = 1, \dots, n \ . \tag{10}$$

For inert components of the reaction mixture both their net flux densities and stoichiometric coefficients equal zero. Thus, it is possible to write Eq. (*5*) in the form of following constitutive equations

$$\frac{\mathrm{d}c_i}{\mathrm{d}z} = \frac{N_1}{D_i} \ , \quad i = 1, \dots, n \tag{11}$$

with the (formal) global diffusivities D_i defined as

$$\frac{1}{D_i} = \sum_{j=1}^{n} \frac{a_j}{a_1} f_{ij} \ , \quad i = 1, \dots, n \ . \tag{12}$$

Similarly, from the Fourier law,

$$\frac{\mathrm{d}\theta}{\mathrm{d}z} = \frac{Q}{\lambda T_s} \ . \tag{13}$$

Under steady-state conditions, the mass flux of the key reactant (*e.g.*, A_1) across a boundary surface surrounding a portion of the porous structure equals the amount re-

acted within this portion. The released reaction heat must all be transferred across the same boundary, *i.e.*,

$$Q = N_1(-\Delta H_r)/a_1 \ . \tag{14}$$

Thus,

$$\frac{d\theta}{dz} = \frac{N_1}{D_{n+1}} \tag{15}$$

with

$$\frac{1}{D_{n+1}} = \frac{-\Delta H_r}{\lambda T_s a_1} \ . \tag{16}$$

From Eqs (*11*), (*12*), (*15*), and (*16*) it follows that the relations between concentrations of non-key components (A_2,…, A_n) and the key component (A_1), $c_i = c_i(c_1)$, and dimensionless temperature and concentration of the key component, $\theta(c_1)$, are described by the set of first-order ordinary differential equations (*17*)

$$\frac{dc_i}{dc_1} = \frac{D_1}{D_i} \ , \quad i = 2, ..., n$$
$$\frac{d\theta}{dc_1} = \frac{D_1}{D_{n+1}} \ , \tag{17}$$

with boundary conditions describing the situation at the outer surface of the catalyst pellet

$$\text{for } c_1 = c_{1s}: \quad c_i = c_{is} \ , \quad i = 2, ..., n$$
$$\theta = 1 \tag{18}$$

By integrating the initial value problem (*17*) from $c_1 = c_{1s}$ to $c_1 = 0$ (in case of incomplete disappearance of the key component A_1 under equilibrium conditions, to $c_1 = c_1^{eq}$), the mutual dependences $c_i(c_1)$ ($i = 2, …, n$) and $\theta(c_1)$ are obtained. Obviously, the total molar concentration, c, can be obtained as

$$c = \sum_{j=1}^{n} c_j \ . \tag{19}$$

For perfect gases, the pressure, p, follows as $p = cR_gT$. Numerous preliminary calculations have shown that the dependences $c_i(c_1)$ and $\theta(c_1)$ are monotonous and nearly linear and thus can be easily approximated by low-order polynomials.

Second Step

In the course of integration of system (*17*), it is easy to evaluate simultaneously the global diffusivity D_1 as a function of c_1; $D_1(c_1)$. Because of the monotonous nature of this dependence, it is easy to approximate $D_1(c_1)$, *e.g.*, by a low-order polynomial. Then, it is feasible to use directly the second-order ordinary differential equation obtained by elimination of N_1 between the mass balance (*2*), (for $i = 1$), and constitutive equations (*11*). With the following definitions

$$u \equiv \frac{c_1}{c_{1s}} \quad \Delta \equiv \frac{D_1}{D_{1s}} \quad \rho \equiv \frac{R_1}{R_{1s}} \quad x \equiv \frac{z}{R} \ , \tag{20}$$

this ordinary differential equation can be written as

$$\frac{d^2u}{dx^2} + \frac{w}{x}\frac{du}{dx} + \left(\frac{du}{dx}\right)^2 \Phi = M^2 \frac{\rho}{\Delta} \ , \tag{21}$$

where the generalized Thiele modulus M is given as

$$M^2 \equiv R^2 \frac{-R_{1s}}{c_{1s} D_{1s}} \ , \tag{22}$$

and Φ characterizes the concentration dependence of the global effective diffusivity, D_1, on c_1:

$$\Phi \equiv \frac{d \ln (\Delta)}{du} \ . \tag{23}$$

R_{1s} is the rate of key-component formation for concentrations and temperature at the outer surface of the catalyst pellet, $R_{1s} = R_1(c_s, \theta = 1)$. Similarly, D_{1s}, is the global diffusivity at the catalyst outer surface, $D_{1s} = D_1(c_s, \theta = 1)$.

Boundary conditions to be used with Eq. (*21*) are

$$\text{at } x = 0 \quad \mathrm{d}u/\mathrm{d}x = 0 \ ,$$
$$\text{at } x = 1 \quad u = 1 \ , \tag{24}$$

i.e., a split boundary value problem for one second-order ordinary differential equation must be solved. From the obtained profile $u(x)$, *i.e.*, $c_1(z)$ and the dependences $c_i(c_1)$ ($i = 2,\ldots, n$), and $\theta(c_i)$, determined in the first step, it is possible to calculate $R_1(z)$.

The catalyst effectiveness factor, η, defined in the usual way as the ratio of the amount of reactant actually reacted in the catalyst pellet to the amount which would react under conditions without mass and heat transport resistance, can be determined by integration of local rates of key-component reaction, R_1, over the whole pellet

$$\eta = \frac{w+1}{R^{w+1}} \int_0^R z^w \frac{R_1}{R_{1\mathrm{s}}} \, \mathrm{d}z = (w+1) \int_0^1 x^w \rho \, \mathrm{d}x \ . \tag{25}$$

EXAMPLE: AMMONIA SYNTHESIS

The general formulation developed above will be illustrated with the case of ammonia synthesis

$$\mathrm{N}_2 + 3 \, \mathrm{H}_2 = 2 \, \mathrm{NH}_3 \tag{A}$$

($A_1 \equiv \mathrm{N}_2$; $A_2 \equiv \mathrm{H}_2$; $A_3 \equiv \mathrm{NH}_3$; the presence of an inert gas, A_4 (*e.g.*, Ar), is assumed: hence, $n = 4$). The stoichiometric coefficients are: $a_1 = -1$; $a_2 = -3$; $a_3 = 2$; $a_4 = 0$.

The first attempts in the field of effectiveness factor in ammonia synthesis were summarized by Nielsen[9]. More realistic formulations were used later by Dyson and Simon[10], Sing and Saraf[11] and Szeifert *et al.*[12].

First Step

The global diffusivities D_1, D_2, D_3, D_4 and D_5 are defined by Eq. (*12*) using F matrix elements, f_{ij}, given in the Appendix 1 for MTPM and DGM.

The set of coupled ordinary differential equations for relations between concentrations and temperature, and concentration of the key component, $c_2(c_1)$, $c_3(c_1)$, $c_4(c_1)$, $\theta(c_1)$, has the following form

$$\frac{\mathrm{d}c_2}{\mathrm{d}c_1} = \frac{D_1}{D_2} \quad \frac{\mathrm{d}c_3}{\mathrm{d}c_1} = \frac{D_1}{D_3} \quad \frac{\mathrm{d}c_4}{\mathrm{d}c_1} = \frac{D_1}{D_4} \quad \frac{\mathrm{d}\theta}{\mathrm{d}c_1} = \frac{D_1}{D_5} \ . \tag{26}$$

The total molar concentration, c, equals the sum of molar concentration of reaction mixture components: $c = c_1 + c_2 + c_3 + c_4$.

The set of ordinary differential equation is integrated from $c_1 = c_{1s}$ (where $c_2 = c_{2s}$; $c_3 = c_{3s}$; $c_4 = c_{4s}$; $\theta = 1$) to c_1 equal to zero or to equilibrium value, c_1^{eq}. Substitution of the current variables (c_i, θ) into the equilibrium condition of ammonia synthesis[13],

$$K_p(T) - \frac{c_3^2}{c_1 c_2^3} c_\oplus^2 = 0 \ , \qquad (27)$$

can check attaining equilibrium conditions in each integration step ($c_\oplus$ denotes the molar concentration in the standard state of gases, *i.e.*, at system temperature and pressure 101.325 kPa). When this condition is fulfilled, further integration can be stopped. During the integration, the dependence of global diffusivity, D_1, on the molar concentration of the key component, c_1, is evaluated. D_1 for conditions at the outer surface of the catalyst pellet, D_{1s}, is determined by substitution of the surface values of variables into D_1 definition.

The dependences $c_2(c_1)$, $c_3(c_1)$, $c_4(c_1)$, $\theta(c_1)$, $D_1(c_1)$, obtained for MTPM and parameters summarized in Table I are shown in Figs 1 and 2. It can be seen that straight lines are obtained for $c_i(c_1)$ ($i = 2, \ldots, 4$) as well as for $\theta(c_1)$ and $D_1/D_{1s}(c_1)$.

Also shown in Fig. 1 is a slight dependence of the relative total pressure on concentration of the key component, c_1. As expected, the total pressure decreases in the direc-
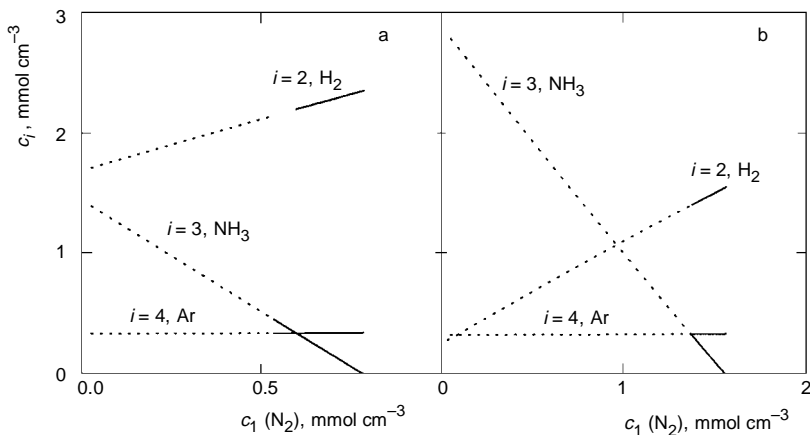
FIG. 1

Concentration dependences for ammonia synthesis at 700 K and 19.78 MPa (*i.e.*, 200 atm) according to MTPM. $A_1 \equiv N_2$; $A_2 \equiv H_2$; $A_3 \equiv NH_3$; $A_4 \equiv Ar$. Bulk gas composition $N_2/H_2/NH_3/Ar$ (vol.%): a (stoichiometric ratio $N_2/H_2 = 1/3$) – 22.5/67.5/0/10; b (equimolar ratio $N_2/H_2 = 1/1$) – 45/45/0/10. Dotted lines show unattainable concentrations above reaction equilibrium

tion toward the pore end, *i.e.*, with decreasing c_1. Owing to the large mean transport-pore size ($\langle r \rangle$ = 100 nm), the Knudsen transport contribution is minor and the effective permeability quite high. Thus, small total pressure gradients suffice to produce permeation fluxes of reaction mixture components.

TABLE I
Parameters for effectiveness factor calculations

Parameter	Value
Temperature	700 K
Pressure	19.78 MPa (*i.e.*, 200 atm)
Mean transport-pore radius, $\langle r \rangle$	100 nm
Mean of squared transport pore radii, $\langle r^2 \rangle$	10 000 nm^2
Geometric parameter, ψ	0.1
Binary bulk diffusivities, D_{ij}^{m}	estimated refs[21,22]
Catalyst effective thermal conductivity, λ	0.001 J cm^{-1} s^{-1} K^{-1}
Reaction enthalpy, ΔH_r	–92.1 kJ mol^{-1}
Pellet shape, w (sphere)	2
Pellet radius, R	0.3 cm
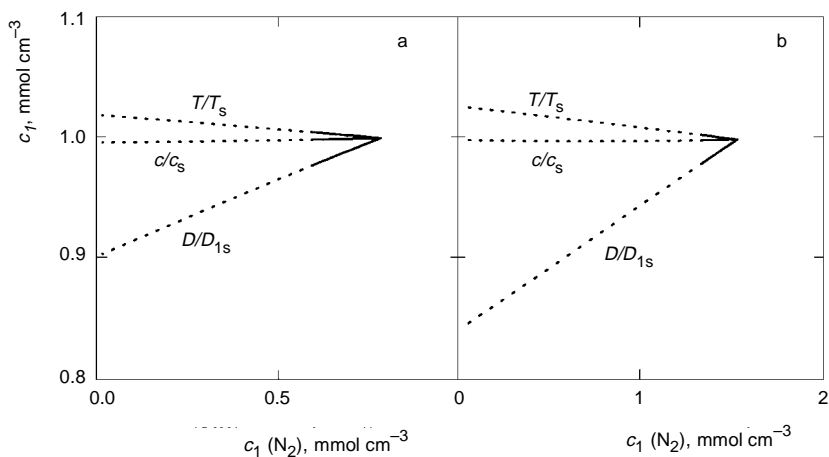
FIG. 2
Dependences of temperature (T/T_s), total pressure (c/c_s) and global diffusivity (D_1/D_{1s}), on c_1 for ammonia synthesis at 700 K and 19.78 MPa (*i.e.*, 200 atm) (MTPM). $A_1 \equiv N_2$; $A_2 \equiv H_2$; $A_3 \equiv NH_3$; $A_4 \equiv Ar$. Bulk gas composition $N_2/H_2/NH_3/Ar$ (vol.%): **a** (stoichiometric ratio N_2/H_2 = 1/3) – 22.5/67.5/0/10; **b** (equimolar ratio N_2/H_2 = 1/1) – 45/45/0/10

Contrary to expectation, for a reaction accompanied by a decrease in the number of moles, DGM predicts a slight total pressure *increase* with decreasing c_1. This is even more marked for smaller pores. For $\langle r \rangle = 5$ nm and the equimolar concentration ratio of nitrogen and hydrogen in the bulk gas, DGM predicts 21.48 MPa (*i.e.*, 212 atm) at the place in the pore where nitrogen is completely exhausted. In agreement with expectation, MTPM predicts for the same conditions 19.86 MPa (*i.e.*, 196 atm). Therefore, the following calculations were performed with MTPM only.

By using the published[13] standard Gibbs energy change of reaction (*1*), ΔG_r^0, the equilibrium constant, K_p, was determined from $-\Delta G_r^0 = R_g T \ln (K_p)$. Application of Eq. (*27*) then permitted to determine the reaction mixture compositions inside the pores which are below equilibrium (full lines in Fig. 1). Obviously, compositions for which the reaction equilibrium is exceeded (dotted lines in Fig. 1) cannot be reached. The attainable composition intervals are very narrow, which points to a significant role of reaction equilibrium in the ammonia synthesis. It can be also seen that hydrogen concentration decreases much less than nitrogen concentration even though the bulk gas at the pore entrance contains the stoichiometric ratio of components. Argon concentration inside the pores remains nearly the same as in the bulk gas, similarly as the total molar concentration (pressure).

Second Step

If the kinetic equation of the reaction is known, then the approximations for $c_2(c_1)$, $c_3(c_1)$, $c_4(c_1)$, $\theta(c_1)$ and $D_1(c_1)$ can be used for evaluation of Δ and ρ (Eq. (*20*)) and the derivative $d \ln (\Delta)/du$ (Eq. (*23*)) as functions of u (*i.e.*, dimensionless c_1). The Thiele modulus, M (Eq. (*22*)), is determined from the pellet surface conditions. The integration of the mass balance (*21*) with split boundary conditions (*24*) is performed *via* any suitable numerical algorithm (*e.g.*, a shooting method).

Since the Temkin–Pyzhev rate equation (see, *e.g.*, refs[10–12,14,15]) is inapplicable to the inlet of a packed bed catalytic reactor where the reaction mixture is free of ammonia, an equation of the form suggested, *e.g.*, by Thomas and Thomas[16] was used

$$r = \frac{k(p_1 - p_1^*)/p_\oplus}{\left[1 + K\left(\dfrac{p_\oplus^{0.5} p_3}{p_2^{1.5}}\right)\right]^2} \ . \tag{28}$$

Here p_i are the component partial pressures, $p_\oplus = 101.325$ (dimensionless) and p_1^* denotes nitrogen partial pressure in equilibrium with other reaction mixture components,

$$p_1^* = p_\oplus^2 p_3^2 /(p_2^3 K_p) \ . \tag{29}$$

The constants k and K in the form

$$k = k_0 \exp\left[A\left(\frac{1}{T} - \frac{1}{700}\right)\right] ,$$

$$(30)$$

$$K = K_0 \exp\left[B\left(\frac{1}{T} - \frac{1}{700}\right)\right] ,$$

were obtained by matching the high-pressure experimental data of Nielsen[14] for temperatures 410–500 °C. The following values were obtained: $k_0 = 395$ mmol s^{-1} MPa^{-1} cm$_{\text{pellet}}^{-3}$, $A = 8.2396$ K^{-1}, $K_0 = 260.8$ MPa$^{1/2}$, $B = 3\,470.7$ K^{-1}.

Using this rate equation, the profile of attainable key component concentration $c_1(x)$ is obtained. By combining $c_1(x)$ with approximations $c_2(c_1)$, $c_3(c_1)$, $c_4(c_1)$ and $\theta(c_1)$, it is possible to determine the concentration profiles of all the reaction mixture components, $c_i(x)$, as well as the temperature profile $T(x)$. From Fig. 3 it can be seen that for hydrogen, nitrogen and argon these profiles are only very slightly curved (note the scale of c_1, c_2 and c_4 axes). Only the ammonia profile is more pronounced. The temperature profile, $T(x)$, is not shown as the calculations only predict an increase of 0.2 K in the pellet centre.

The profile of local reaction rates for the stoichiometric N_2/H_2 mixture containing no ammonia and 10% argon are shown in Fig. 4 for 700 K and 19.78 MPa (*i.e.*, 200 atm). The profile is very steep near the pellet outer surface showing that the main proportion of the reaction takes place in a shallow outside layer of the catalyst pellet. The effec-
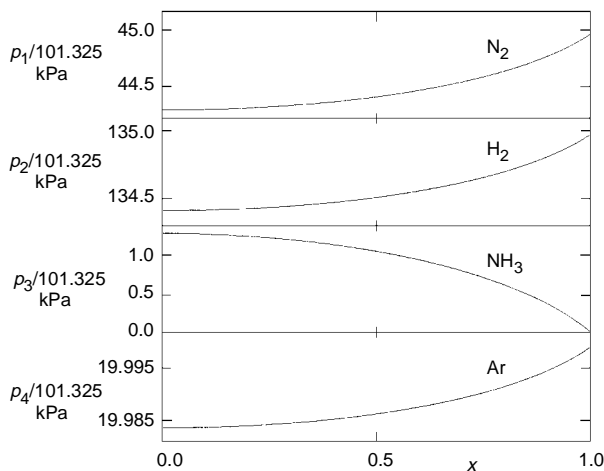
Fig. 3
Partial pressure profiles, ($p_i(x)$, i = 1–4), inside a porous catalyst for ammonia synthesis at 700 K and 19.78 MPa (*i.e.*, 200 atm) (MTPM). $A_1 \equiv N_2$; $A_2 \equiv H_2$; $A_3 \equiv NH_3$; $A_4 \equiv Ar$. Bulk gas composition $N_2/H_2/NH_3/Ar$ (vol.%): (stoichiometric ratio N_2/H_2 = 1/3) – 22.5/67.5/0/10. (Partial pressures, $p_i = c_i R_g T$, are used instead of molar concentrations c_i.)

tiveness factor, η, calculated according to Eq. (*25*) equals 30.8%. As a rough comparison, Dyson and Simon[10] predict for similar conditions $\eta = 13\%$.

The problem of the effectiveness factor for ammonia synthesis combines the differing transport rates of reaction mixture components, which make the composition inside pores quite different from the bulk gas composition, with the unfavourable reaction equilibrium. To look further into this problem, the effectiveness factors for the inlet of a packed-bed reactor (*i.e.*, with no ammonia presence in the bulk gas) was calculated for different nitrogen/hydrogen ratios. The results are presented in Fig. 5 which shows the sensitivity of η to this factor.

Another example, shown in Fig. 6, illustrates the sensitivity of η to the content of ammonia in the bulk gas. Along a packed bed reactor, in which nitrogen and ammonia are consumed and ammonia is produced, the effectiveness factor increases from the lowest value at the reactor entrance ($\eta = 30.8\%$) to nearly 100% when a 5% conversion is reached. However, at this point, the reaction mixture is close to thermodynamic
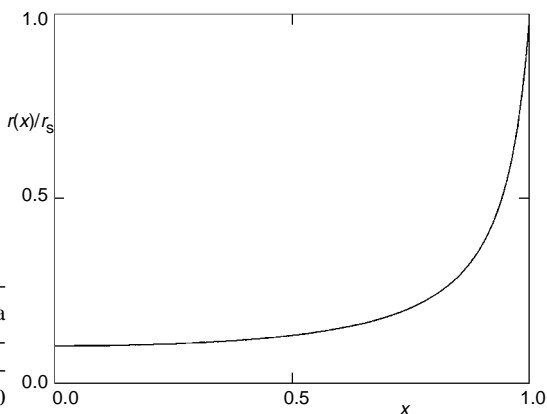
Fig. 4

Profile of local reaction rates for ammonia synthesis at 700 K and 19.78 MPa (*i.e.*, 200 atm) (MTPM). Bulk gas composition $N_2/H_2/NH_3/Ar$ (vol.%): (stoichiometric ratio $N_2/H_2 = 1/3$) – 22.5/67.5/0/10
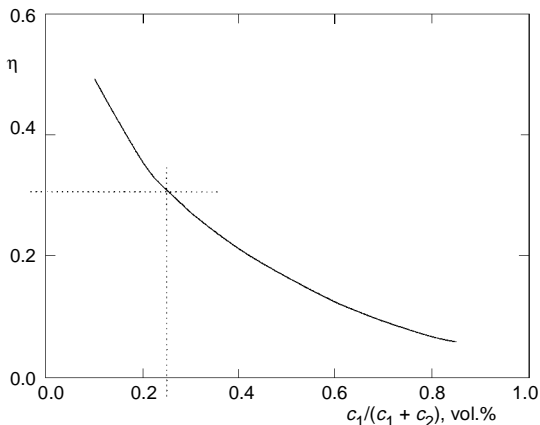
Fig. 5

Influence of nitrogen mole fraction in the bulk gas on the effectiveness factor for ammonia synthesis at 700 K and 19.78 MPa (*i.e.*, 200 atm) (MTPM). Bulk gas contains no ammonia and 10% Ar. Dotted lines show the effectiveness factor for stoichiometric N_2/H_2 mixture

equilibrium and hence the reaction rate is nearly zero; the mass and heat transport, then, play no role.

CONCLUSIONS

The suggested two-step procedure for determination of catalyst effectiveness factor for stoichiometrically simple reactions removes the necessity of solving the boundary value problem for sets of coupled non-linear differential equations. At the same time, a deeper insight into the concentration and temperature conditions inside the pores is gained. Information of this kind can cast light on some features of catalytic reactor behaviour. An analysis of the ammonia synthesis illustrates this point.

APPENDIX 1

Matrix F

The modified Maxwell–Stefan equation can be used for relating the molar flux densities, N_i, to molar concentration gradients.

The actual form of dependences of f_{ij} on c_i and parameters that characterize the pore structure of the catalyst, depends on the way the pore structure is modelled and on the applied physical description of individual mass transport processes taken into account.

The mean transport-pore model (MTPM, refs[17–19]) visualizes that part of the pore structure through which the decisive part of mass transport takes place as a bundle of straight cylindrical non-intersecting capillaries with radii distributed around the mean $\langle r \rangle$ (mean transport-pore radius, model parameter). The distribution of pore radii is characterized through the mean squared transport-pore radius $\langle r^2 \rangle$ (model parameter). The fact that not necessarily all pores are active in mass transport is expressed in the third model
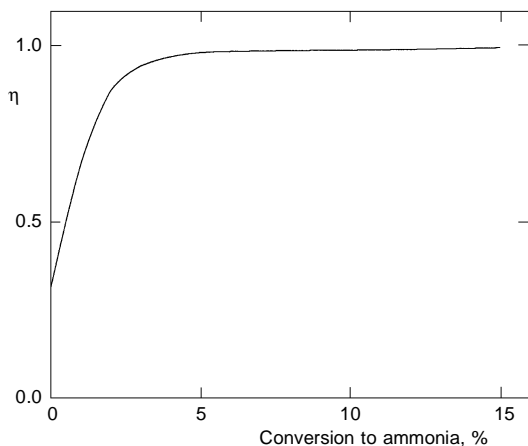
Fig. 6
Change of the effectiveness factor with bulk gas conversion to ammonia (770 K, 19.78 MPa, *i.e.*, 200 atm) (MTPM). Stoichiometric ratios of N_2, H_2 and NH_3 in the bulk gas; at zero conversion, the bulk gas contains 10% Ar

parameter, ψ, which combines the porosity of transport pores, ε, with their tortuosity, q: $\psi = \varepsilon/q$. These parameters are the material constants of the porous medium described by MTPM and have to be obtained experimentally.

When these model assumptions are combined with the Maxwell–Stefan equation for multicomponent diffusion in the transition region between Knudsen diffusion and molecular diffusion, and modified Darcy equation (see Appendix 2) for gas mixture permeation, the elements f_{ij} of matrix $\boldsymbol{F}$ in Eq. (5) have the form

$$f_{ii} = \frac{1}{D_i^{\mathrm{k}}} + \frac{\alpha_i c_i}{cD_i^{\mathrm{k}}} + \sum_{\substack{j=1 \\ j \neq i}}^{n} \frac{c_j}{cD_{ij}^{\mathrm{m}}} \ , \quad i = 1, ..., n \tag{A1.1}$$

$$f_{ij} = c_i \left(\frac{\alpha_i}{cD_j^{\mathrm{k}}} - \frac{1}{cD_{ij}^{\mathrm{m}}} \right), \quad i, j = 1, ..., n; \quad i \neq j$$

where

$$\alpha_i = \frac{1 - \dfrac{B_i}{D_i^{\mathrm{k}}} - \sum\limits_{\substack{j=1 \\ j \neq i}}^{n} \dfrac{c_j(B_i - B_j)}{cD_{ij}^{\mathrm{m}}}}{\sum\limits_{j=1}^{n} \dfrac{c_j B_j}{cD_j^{\mathrm{k}}}} \ , \quad i = 1, ..., n \ . \tag{A1.2}$$

The effective Knudsen diffusion coefficient of component i, D_i^{k}, and the effective binary molecular diffusion coefficient of pair i–j, D_{ij}^{m}, are defined as follows

$$D_i^{\mathrm{k}} = \langle r \rangle \psi K_i \ , \quad D_{ij}^{\mathrm{m}} = \psi D_{ij}^{\mathrm{m}} \ , \tag{A1.3}$$

where D_{ij}^{m} is the molecular diffusivity of pair i–j and

$$K_i = \frac{2}{3} \left(\frac{8R_{\mathrm{g}}T}{\pi M_i} \right)^{1/2} \tag{A1.4}$$

(M_i is the molecular weight of component i).

The dusty-gas model (DGM, refs[8,20]) visualizes the porous medium as a collection of giant spherical molecules (dust particles) kept in space by external force. The motion of gas molecules in the space between dust particles is described by the kinetic theory of gases. The DGM transport parameters k_0 and k_1 appear in the definitions of effective diffusion coefficients D_i^{k} and D_{ij}^{m} (see below). The third transport parameter B_0 characterizes the viscous flow contribution (Appendix 2). Similarly to MTPM, k_0, k_1 and B_0

have to be obtained experimentally for the given porous solid. Formally, DGM parameter k_0 can be identified with the product of MTPM parameters $\langle r \rangle \psi$ and parameter k_1 with ψ. Also, B_0 equals $\langle r^2 \rangle \psi / 8$.

The elements of the DGM matrix $\mathbf{F}, f_{ij}$, are identical with the corresponding elements of the MTPM matrix. The only difference is in the definition of α_i. For DGM it reads

$$\alpha_i = \frac{-\dfrac{B}{D_i^k}}{1 + B \displaystyle\sum_{j=1}^{n} \frac{c_j}{c D_j^k}} \quad , \quad i = 1, ..., n \ . \tag{A1.5}$$

The effective Knudsen diffusion coefficient of component i, D_i^k, and the effective binary molecular diffusion coefficient of pair i–j, D_{ij}^m, are given as

$$D_i^k = k_0 \, K_i \ , \quad D_{ij}^m = k_1 D_{ij}^m \ . \tag{A1.6}$$

APPENDIX 2

Effective Permeability

For MTPM, the permeation contribution to the molar flux density of component i, N_i^f, is given by the modified Darcy equation

$$N_i^f = B_i \frac{c_i}{c} \frac{dc}{dz} \ . \tag{A2.1}$$

Under non-isothermal conditions, the correct driving force in the Darcy relation is

$$\frac{1}{R_g T} \frac{dp}{dx} = \frac{1}{T} \left[T \frac{dc}{dx} + c \frac{dT}{dx} \right] = \frac{dc}{dx} + c \frac{d \ln T}{dx} \ .$$

The assumption that the driving force $c(d \ln T / dx)$ may be neglected can be formulated as

$$c \frac{d \ln T}{dx} \ll \frac{dc}{dx} \quad i.e. \quad \frac{d \ln T}{d \ln c} \ll 1 \quad \Rightarrow \quad \frac{dT}{T} \ll \frac{dc}{c} \ .$$

This means that when the isothermal driving force in the Darcy equation is used, the relative temperature change must be much lower than the relative change in total molar concentration.

As an example, let us consider the following situation: At $p = 20.265$ MPa (*i.e.*, 200 atm) and $T = 700$ K, the total molar concentration $c = 3.48$ mmol cm^{-3}. If $\Delta c = 10\%$ of c and $\Delta T = 10$ K,

then, $dc/c \approx 0.1$ and $dT/T \approx 10/700 = 0.014$. Hence, $dT/T << dc/c$ ($0.014 < 10$), and the condition for neglecting of the temperature driving force is fulfilled.

The effective permeability coefficient for each component, B_i, is expressed by the Weber equation modified for multicomponent mixtures[17,18]

$$B_i = D_i^k \frac{\omega v_i + K n_i}{1 + K n_i} + \frac{\langle r^2 \rangle \psi}{8 \mu} p \ . \qquad (A2.2)$$

Here $\langle r^2 \rangle$ stands for the third parameter of the MTPM to be obtained experimentally. It represents the mean value of the distribution of squared transport-pore radii. Parameter ω is a numerical coefficient ($\omega = 3\pi/16, \pi/3, \ldots$) which depends on the development details of the Weber equation; v_i is the square root of relative molar mass

$$v_i = (M_i/\overline{M})^{1/2} \ , \quad \overline{M} = \sum_{i=1}^{n} y_i M_i \ , \qquad (A2.3)$$

y_i's are the component mole fractions in the n-component gas mixture, $K n_i$ are the Knudsen numbers, $i.e.$, the ratios of molecule mean free-path lengths, λ_i, to pore diameter. The problem of obtaining the mean free-path length of a component in a multicomponent mixture was analysed earlier[17].

Usually, the permeability measurements performed on porous solids result in effective permeabilities which depend linearly on pressure. This situation is in agreement with the Weber equation both for very high or very low values of the Knudsen number. In case of coarse pores of the promoted iron catalyst, the Knudsen numbers are evidently very low. Hence, the following linear dependences $B_i(p)$

$$B_i = D_i^k \omega v_i + \frac{\langle r^2 \rangle \psi}{8 \mu} p \qquad (A2.4)$$

were used in the present calculations instead of the full Weber equation ($A2.3$).

In DGM, only the viscous contribution to the net permeability flux is considered. Hence,

$$N_i^f = B \frac{c_i}{c} \frac{dc}{dz} \ , \qquad (A2.5)$$

with the effective permeability coefficient B (identical for all mixture components)

$$B = \frac{B_0 p}{\mu} \ , \qquad (A2.6)$$

where B_0 is the third DGM model parameter. By comparing with MTPM, B_0 can be expressed as $B_0 = \langle r^2 \rangle \psi / 8$.

SYMBOLS

a_i	stoichiometric coefficient of component i
A_i	i-th component of reaction mixture
A	temperature coefficient of ammonia synthesis rate constant k, K^{-1}
B	effective permeability (DGM), $cm^2 s^{-1}$
B	temperature coefficient of ammonia synthesis adsorption coefficient K, K^{-1}
B_i	effective permeability of component i (MTPM), $cm^2 s^{-1}$
B_0	viscous flow parameter (DGM), cm^2
c_i	molar concentration of component i, $mol\ cm^{-3}$
c	total molar concentration, $mol\ cm^{-3}$
$\boldsymbol{c}$	vector of molar concentrations, $mol\ cm^{-3}$
$c_\oplus$	molar concentration in standard state, $mol\ cm^{-3}$
D_i^k	effective Knudsen diffusivity of component i, $cm^2 s^{-1}$
D_{ij}^m	bulk diffusivity of pair i–j, $cm^2 s^{-1}$
D_{ij}^m	effective bulk diffusivity of pair i–j, $cm^2 s^{-1}$
D_i	global diffusivity for component i, $cm^2 s^{-1}$
$\boldsymbol{f}_{ij}$	element of matrix $\boldsymbol{F}$, $s\ cm^{-2}$
$\boldsymbol{F}$	matrix, $s\ cm^{-2}$
ΔG_r^0	standard reaction Gibbs energy per unit reaction (1) turnovers, $J\ mol^{-1}$
ΔH_r	reaction enthalpy per unit reaction (1) turnovers, $J\ mol^{-1}$
k, k_0	rate constants of ammonia synthesis, $mmol\ s^{-1}\ MPa^{-1}\ cm_{pellet}^{-3}$
k_0	DGM parameter, cm
k_1	DGM parameter
K, K_0	adsorption coefficient of ammonia synthesis, $MPa^{1/2}$
Kn_i	Knudsen number for component i
K_i	Knudsen coefficient for component i, cm^{-1}
K_p	equilibrium constant
M_i	molar mass of component i, $g\ mol^{-1}$
$\overline{M}$	mean molar mass of the reaction mixture, $g\ mol^{-1}$
N_i	molar flux density of component i, $mol\ cm^{-2}\ s^{-1}$
$\boldsymbol{N}$	vector of mass and heat flux densities, $mol\ cm^{-2}\ s^{-1}$
n	number of components in reaction mixture
p	gas pressure, kPa
p_i	partial pressure of component i, kPa
p_1^*	equilibrium nitrogen partial pressure
$p_\oplus$	conversion factor between pressure units: 101.325
q	tortuosity of transport pores
Q	heat flux density, $J\ cm^{-2}\ s^{-1}$
r	reaction rate, $mol\ cm^{-3}\ s^{-1}$
$\langle r \rangle$	mean transport-pore radius (MTPM), cm
$\langle r^2 \rangle$	mean of squared transport-pore radii (MTPM), cm^2
R	radius (sphere, infinite cylinder), half width (slab), cm
R_g	gas constant, $J\ mol^{-1}\ K^{-1}$
R_i	rate of formation of component i, $mol\ cm^{-3}\ s^{-1}$

$\boldsymbol{R}$	vector of rates of formation, mol cm^{-3} s^{-1}
T	temperature, K
u	dimensionless key component concentration c_1/c_{1s}
w	pellet shape parameter
x	dimensionless length coordinate z/R
y_i	mole fraction of component i
z	length coordinate of the porous pellet, cm
Δ	dimensionless global diffusivity of key component D_1/D_{1s}
ε	porosity of transport pores
η	effectiveness factor
θ	dimensionless temperature T/T_s
λ	effective thermal conductivity, J cm^{-1} s^{-1} K^{-1}
λ_i	mean free-path length of component i in the reaction mixture, cm
μ	mixture viscosity, Pa s
ν_i	$(M_i/\overline{M})^{1/2}$
ρ	dimensionless reaction rate $= R_1/R_{1s}$
ψ	geometric transport parameter
ω	numerical coefficient

Subscripts

s	conditions at the pellet outer surface
i	reaction mixture component

REFERENCES

1. Thiele E. W.: *Ind. Eng. Chem.* **1939**, *31*, 916.
2. Zeldovitsch Ya. B.: *Acta Physicochim. U.R.S.S.* **1939**, *10*, 583.
3. Wheeler A.: *Adv. Catalysis* **1951**, *3*, 249.
4. Satterfield C. N.: *Mass Transfer in Heterogeneous Catalysts*. MIT Press, Cambridge 1970.
5. Aris R.: *The Mathematical Theory of Diffusion and Reaction in Permeable Catalysts*. Clarendon Press, Oxford 1975.
6. Rothfeld L. B.: *AIChE J.* **1963**, *9*, 19.
7. Jackson R.: *Transport in Porous Catalysts*. Elsevier, Amsterdam 1977.
8. Mason E. A., Malinauskas A. P.: *Gas Transport in Porous Media: The Dusty-Gas Model*. Elsevier, Amsterdam 1983.
9. Nielsen A.: *An Investigation of Promoted Iron Catalyst for the Synthesis of Ammonia*, 2nd ed. Jul. Gjellerups Forlag, Copenhagen 1956.
10. Dyson D. C., Simon J. M.: *Ind. Eng. Chem. Fundam.* **1968**, 7, 605.
11. Singh C. P. P., Saraf D. N.: *Ind. Eng. Chem. Process Des. Dev.* **1979**, *18*, 364.
12. Szeifert F., Arva P., Nagy D., Berty J.: *Hung. J. Ind. Chem.* **1988**, *18*, 287.
13. Malinovsky M., Rousar I.: *Teoreticke zaklady pochodu anorganicke technologie I. Chemicko-inzenyrska termodynamika*. SNTL, Praha 1987.
14. Nielsen A., Kjaer J., Hansen B.: *J. Catal.* **1964**, *3*, 68.
15. Buzzi Ferraris G., Donati G., Rejna F., Carra S.: *Chem. Eng. Sci.* **1974**, *29*, 1621.
16. Thomas J. M., Thomas W. J.: *Introduction to the Principles of Heterogeneous Catalysis*. Academic Press, London 1967.
17. Schneider P.: *Chem. Eng. Sci.* **1978**, *33*, 1311.
18. Fott P., Petrini G., Schneider P.: *Collect. Czech. Chem. Commun.* **1983**, *48*, 215.

19. Schneider P., Gelbin D.: *Chem. Eng. Sci*. **1985**, *40*, 1093.
20. Mason E. A., Malinauskas A. P., Evans R. B.: *J. Chem. Phys*. **1967**, *46*, 3199.
21. Fuller E. N., Schettler P. D., Giddings J. C.: *Ind. Eng. Chem*. **1966**, *58*, 19.
22. Reid R. C., Prausnitz J. M., Poling B. E.: *The Properties of Gases and Liquids*, 4th ed. McGraw–Hill, New York 1988.